

Supporting Information

Minimum Hyaluronic Acid (HA) Modified Magnetic Nanocrystals with Less Facilitated Cancer Migration and Drug Resistance for Targeting CD44 Abundant Cancer Cells by MR Imaging

Taeksu Lee^a, Hye Young Son^b, Yuna Choi^b, Youngmin Shin^b, Seungjae Oh^c, Jinyoung Kim^a, Yong-Min Huh^{b,c,*}, and Seungjoo Haam^{a,*}

^a Department of Chemical and Biomolecular Engineering, Yonsei University, Seoul 120-749, South Korea

^b Department of Radiology, College of Medicine, Yonsei University, Seoul 120-752, South Korea

^c YUHS-KRIBB Medical Convergence Research Institute, Seoul 120-752, South Korea

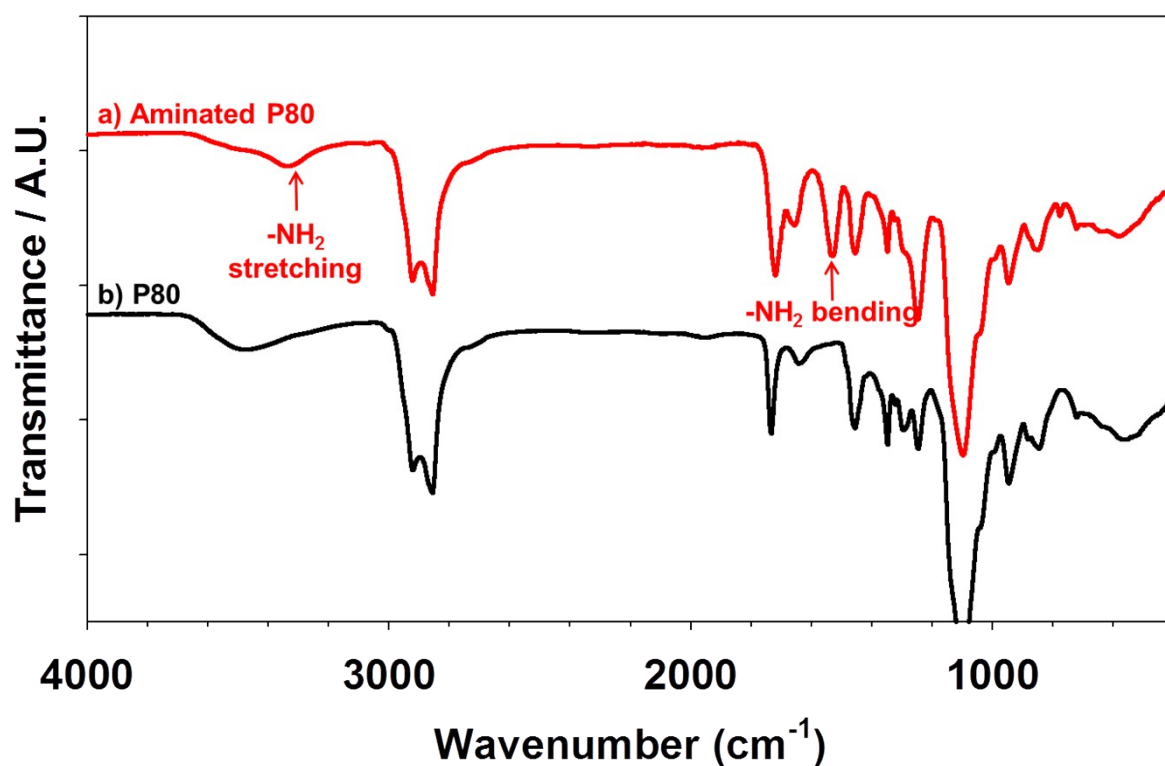


Figure S1. FT-IR spectra of a) aminated P80 (red line) and b) P80 (black line)

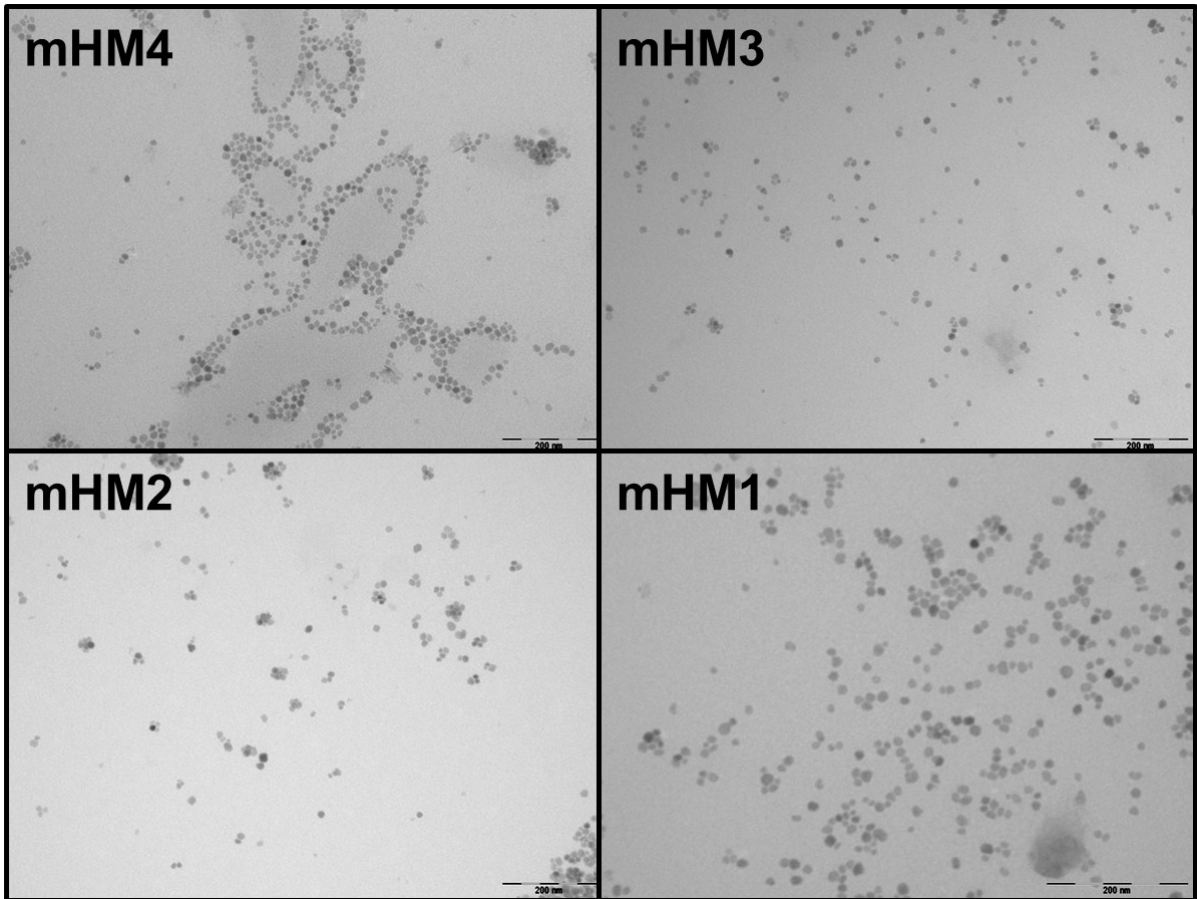


Figure S2. Representative TEM images of mHM 1,2,3,4.

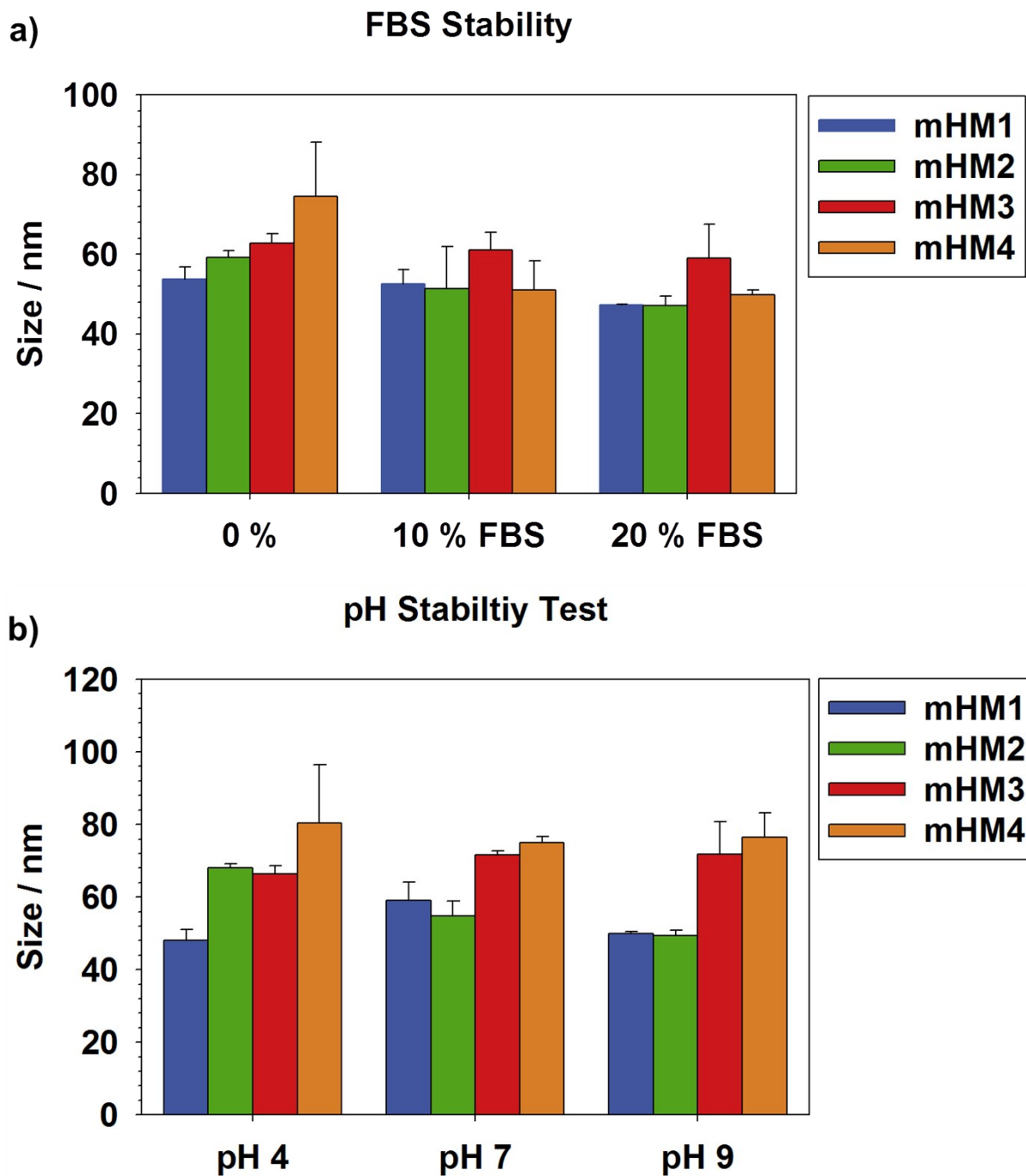


Figure S3. Colloidal stability of mHMs against a) various FBS concentrations (0%, 10%, and 20%) and different pH conditions (pH 4, 7, and 9) for 1 day at room temperature.

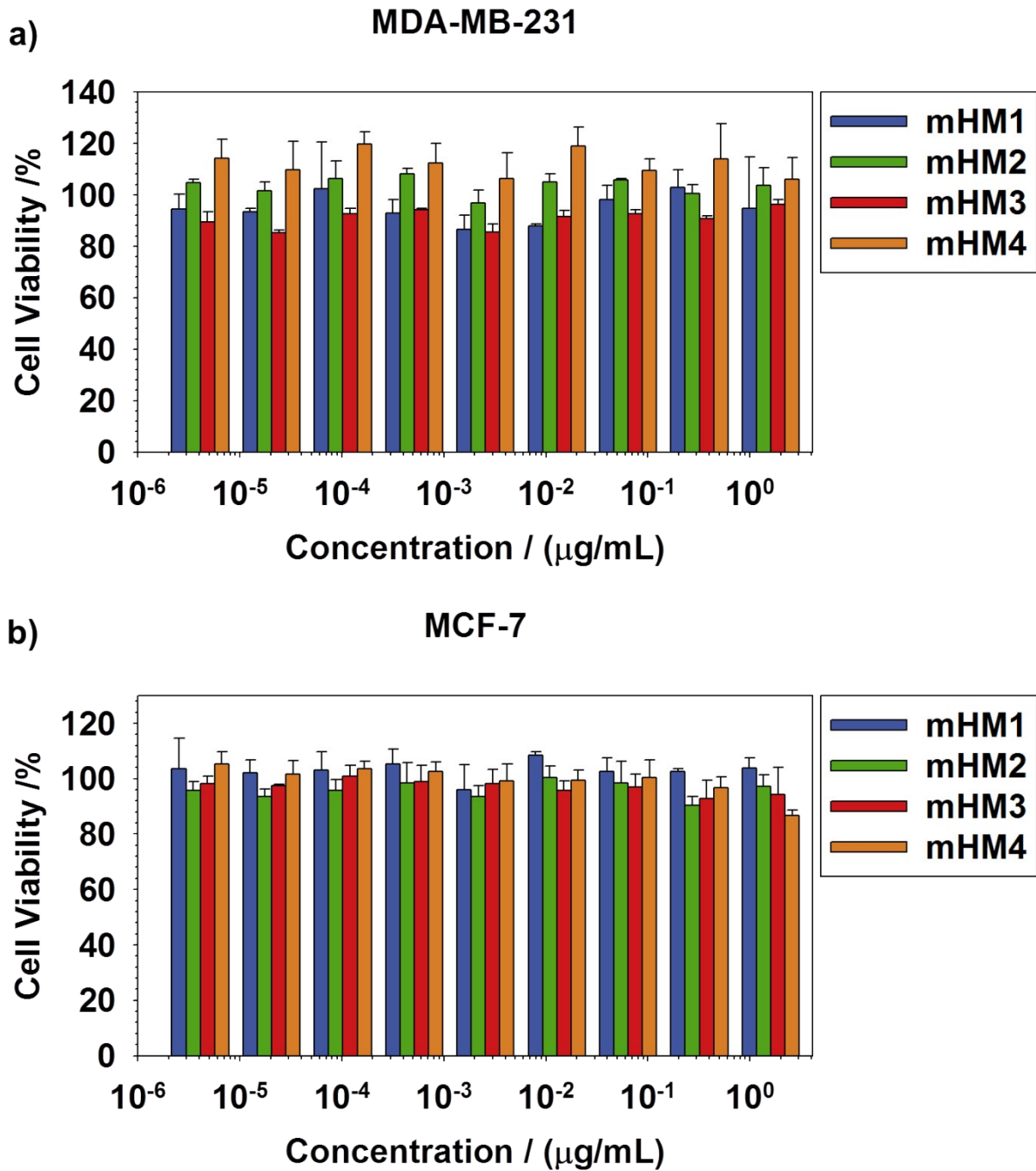


Figure S4. Cell viabilities of a) MDA-MB-231 cells and b) MCF-7 cells (1×10^4 cells each) after incubation with various concentrations of mHMs ($4.1 \times 10^{-6} - 1.6 \mu\text{g/mL}$) for 1 day at 37°C in a 5% CO_2 atmosphere using the 3-(4,5-dimethylthiazolyl-2)-2,5-diphenyltetrazolium bromide (MTT) assay.

5 μg

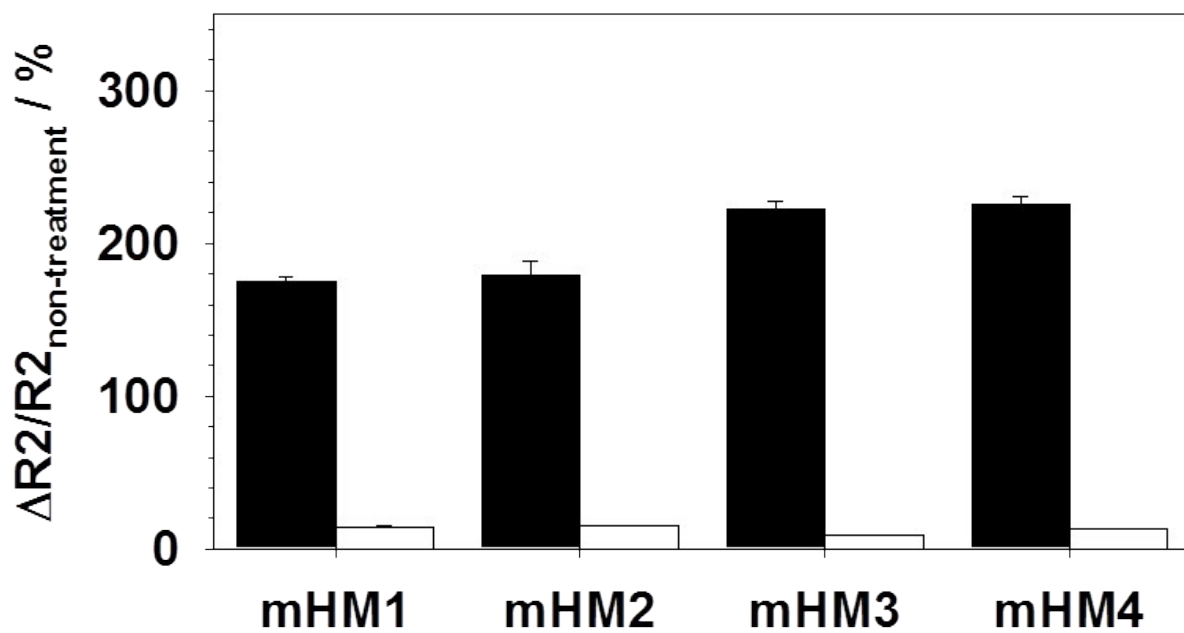


Figure S5. $\Delta R_2/R_{2\text{non-treatment}}$ of MDA-MB-231 (black bar) and MFC-7 (white bar) after mHMs treatment at the 5 μg metal (Fe + Mn) concentration.

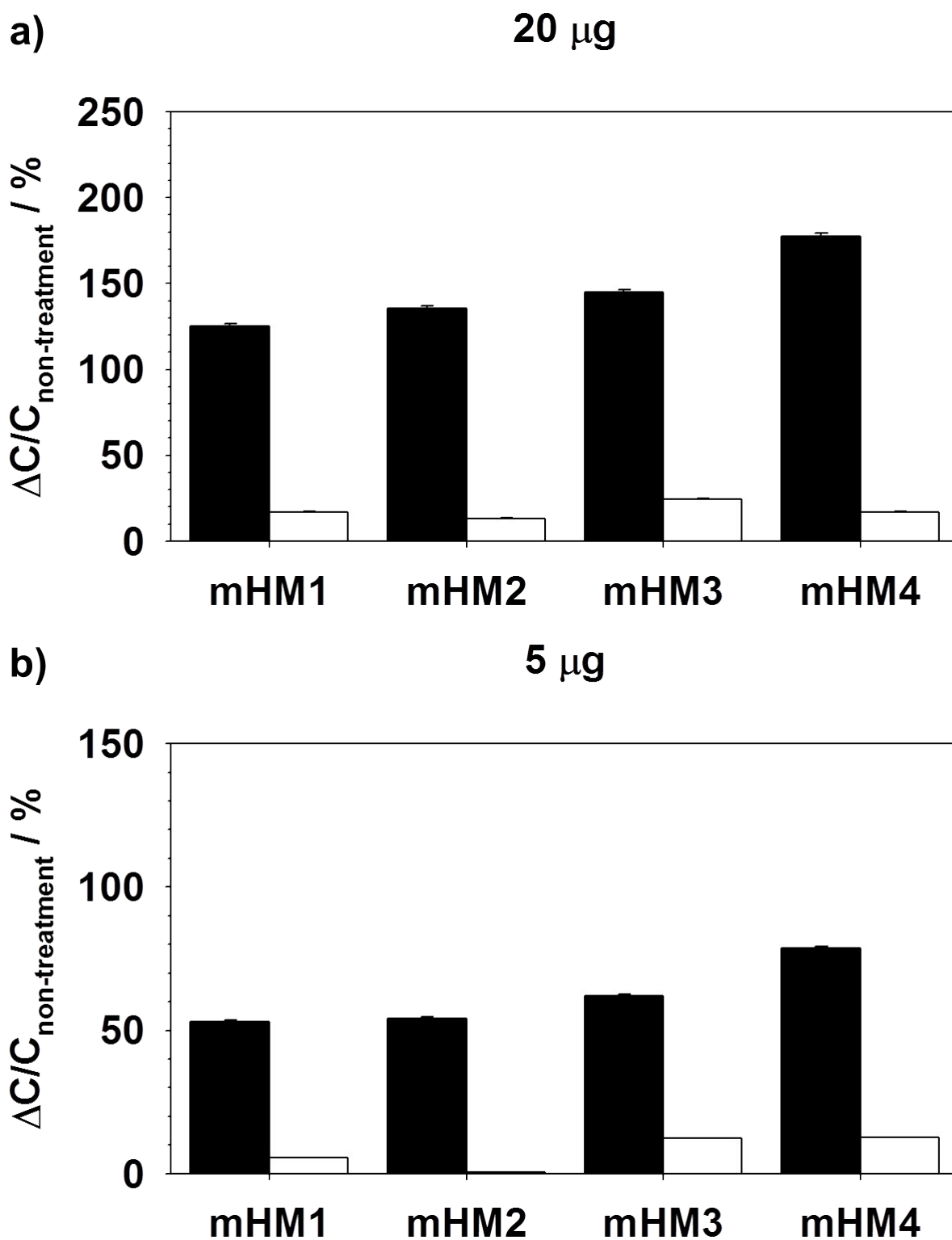


Figure S6. $\Delta C/C_{\text{non-treatment}}$ of MDA-MB-231 (black bar) and MFC-7 (white bar) after mHMs treatment at a) 20 and b) 5 μg metal (Fe + Mn) concentrations.

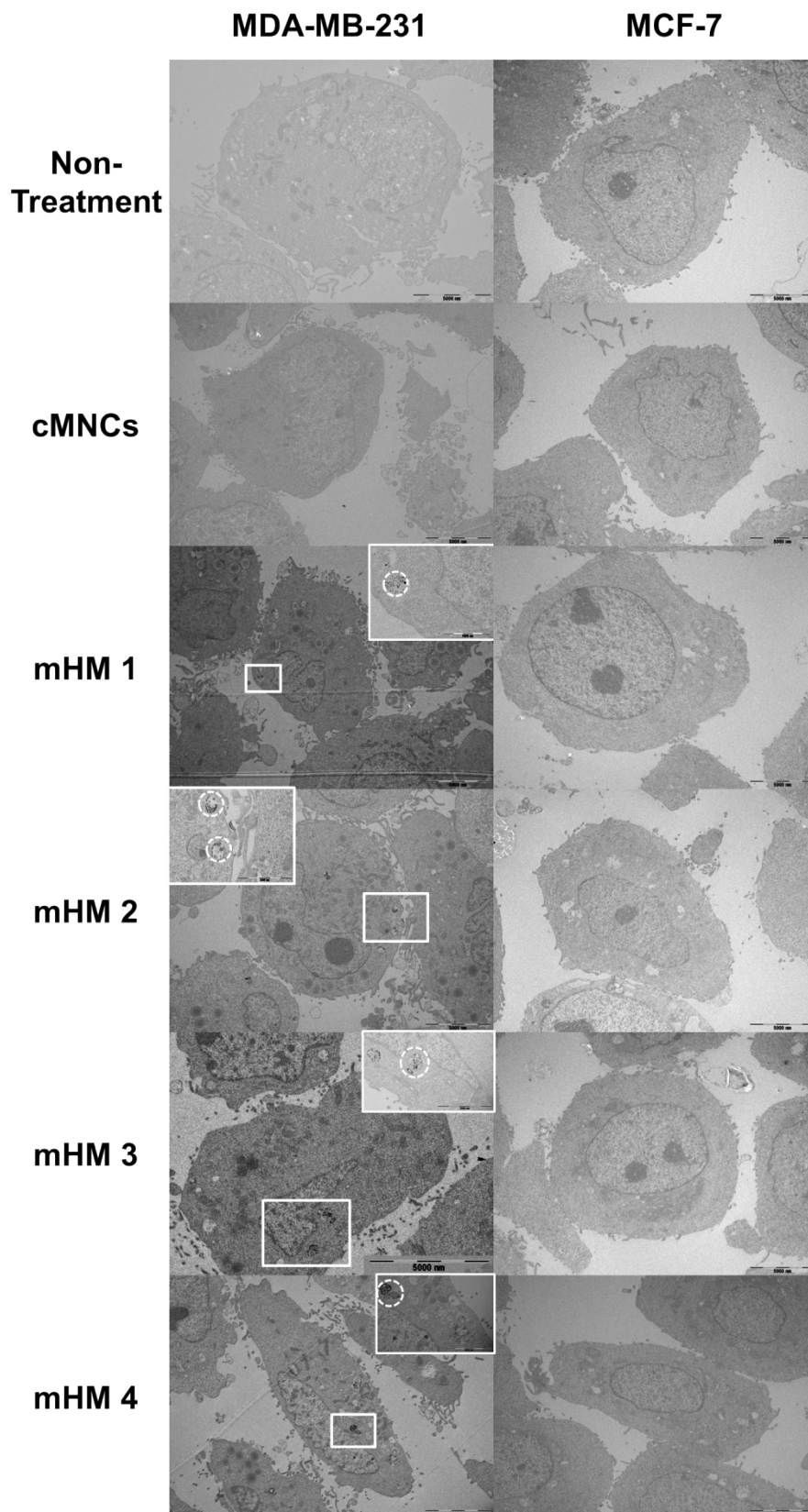


Figure S7. TEM image of MDA-MB-231 and MCF-7 cells incubated with cMNCs and mHMs (inset, magnification of the mHMs in the cytoplasm). The mHMs were internalized via receptor mediated endocytosis.

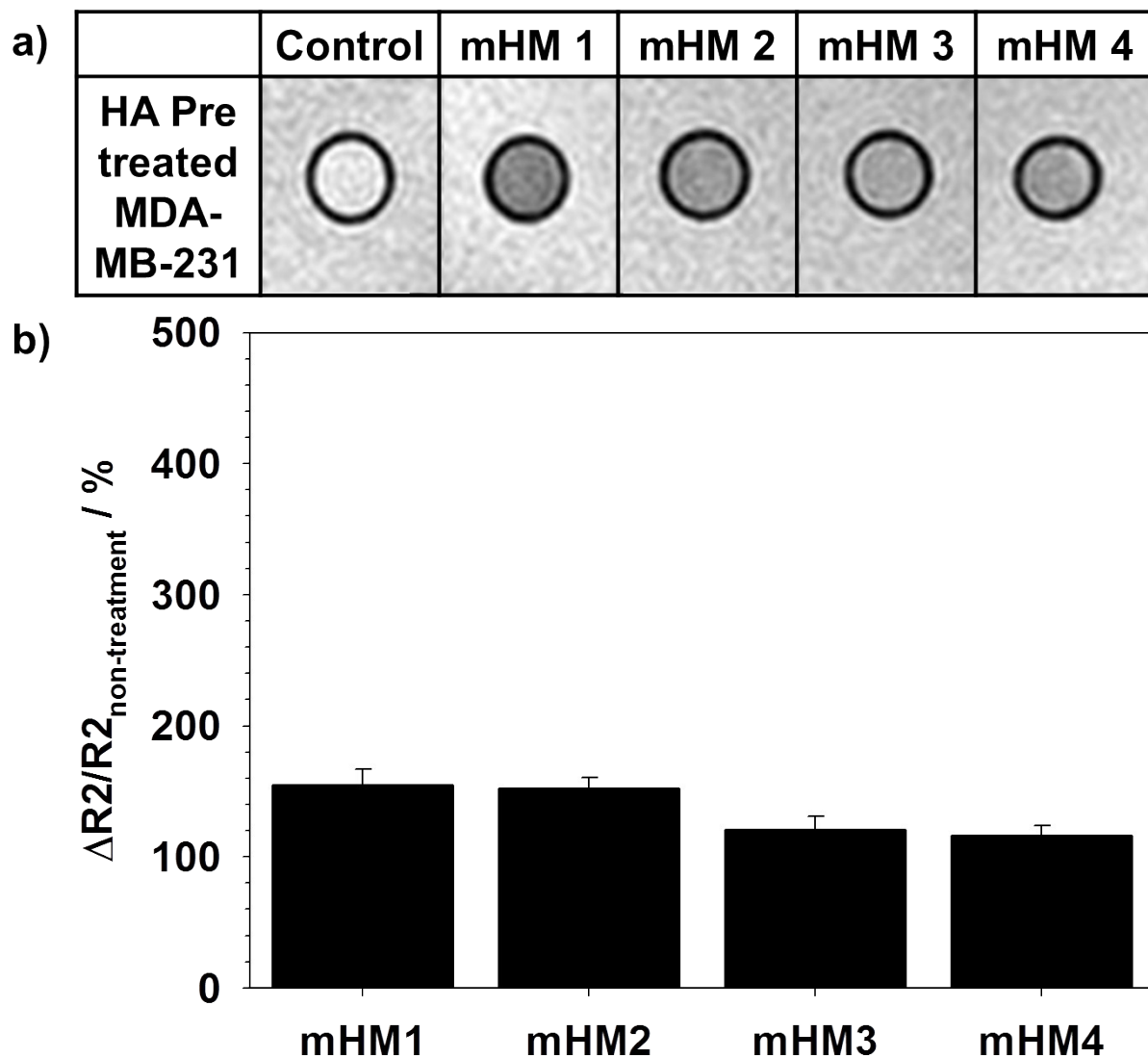


Figure S8. a) T_2 -weighted MR images and b) The graph of $\Delta R_2/R_{2\text{non-treatment}}$ of MDA-MB-231 cells after pre-incubation for 1 day with free HA (1 mg/mL) and treatment with 20 μg of mHM1, 2, 3, 4 and non-treated cells.

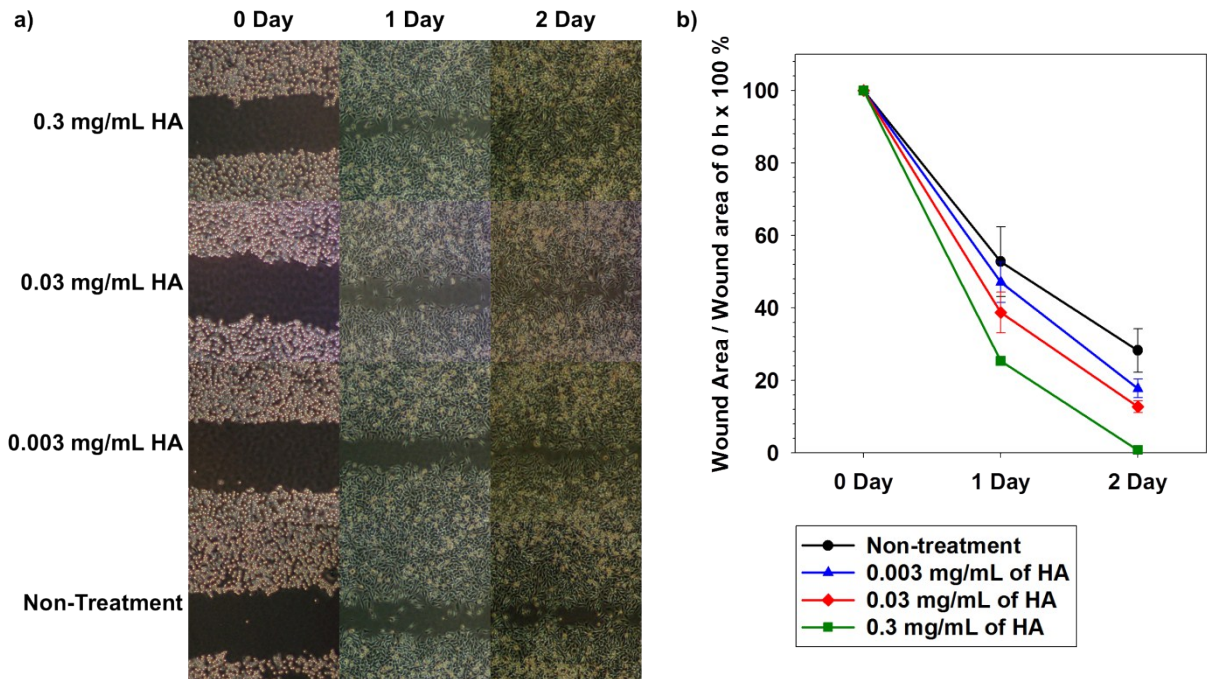


Figure S9. HA facilitated breast cancer cell migration. We performed a wound healing migration assay to determine the motility induction in various concentrations of HA (0.003 mg/mL - 0.3 mg/mL) treated and non-treated MDA-MB-231 cell lines. After seeding of 1×10^6 cells, we wounded the cell monolayer using a sterile pipette tip and washed the cells with PBS. a) Thereafter, cells were photographed at 0, 1, and 2 days using a microscope (Olympus, Japan). b) Quantification was carried out by measuring the wound areas divided by wound area at 0 days.

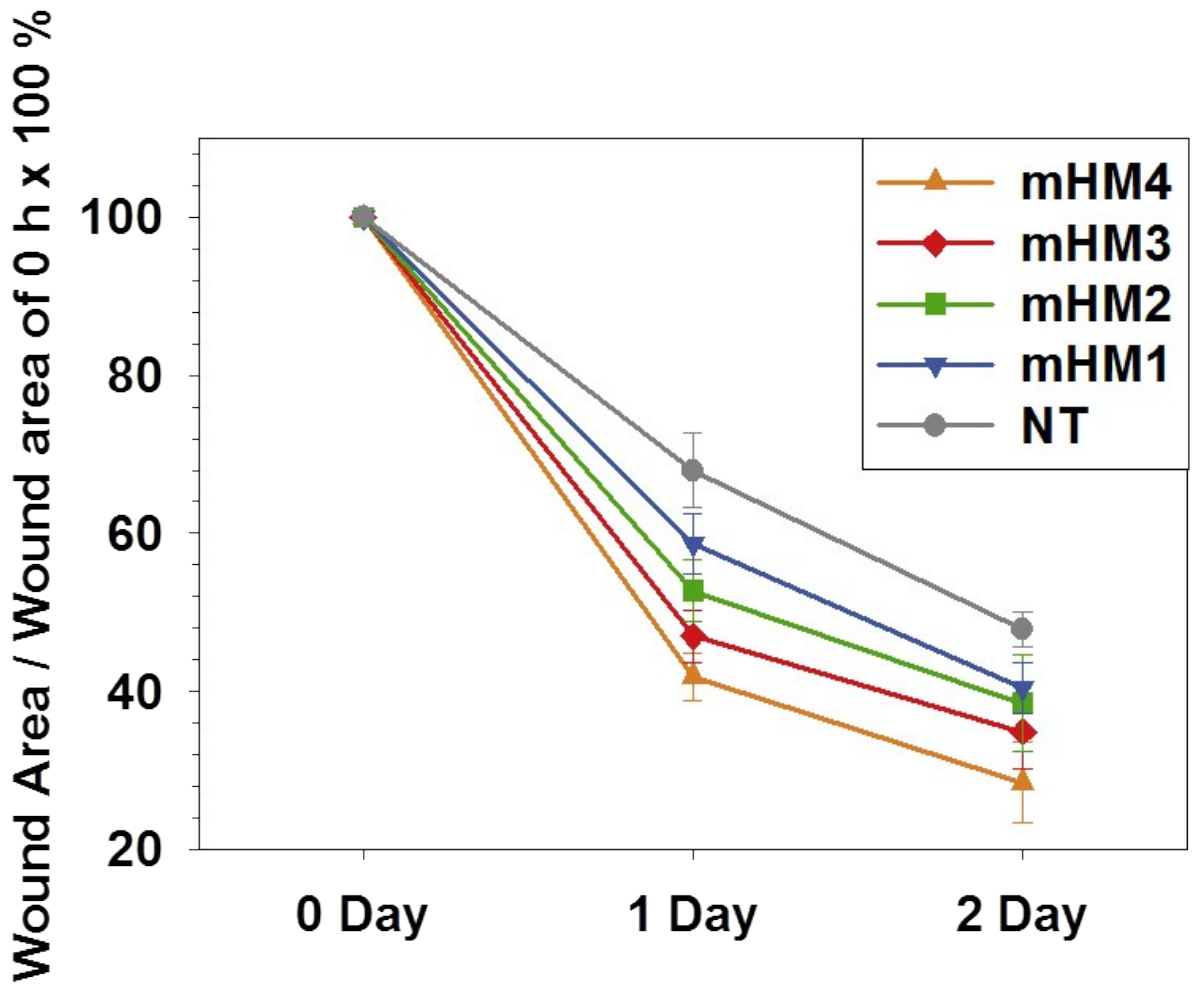


Figure S10. The relative ratio of wound closure per field. The greater the amount of HA conjugated, the faster the migration rate was confirmed. Non-treatment (gray); mHM1 (blue); mHM2 (green); mHM3 (red); mHM4 (orange).

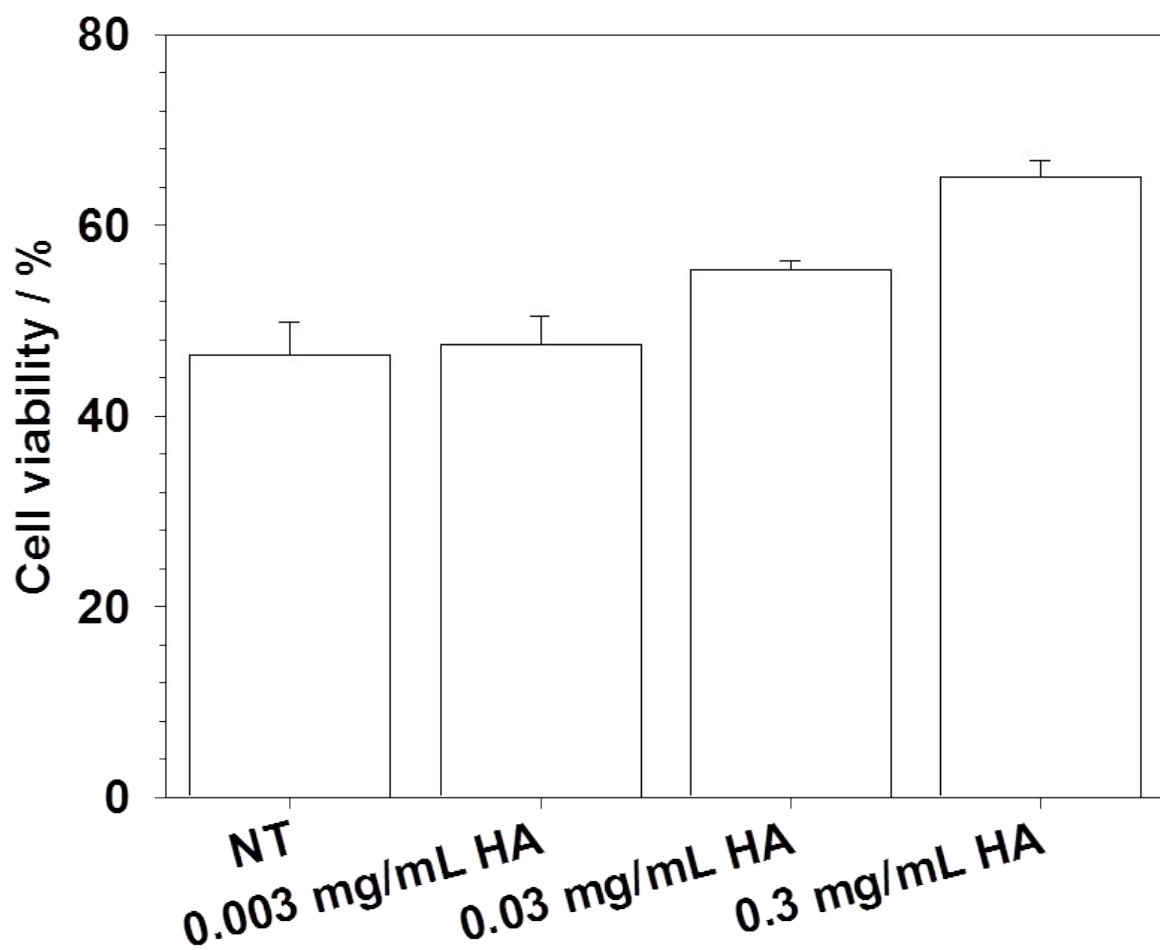


Figure S11. Cell viabilities of MDA-MB-231 cells after treatment with different concentrations of HA and non-treatment, as a control, followed by addition of 25 μ M doxorubicin. After 80 h, the percentages of live cells were analyzed by the MTT assay.

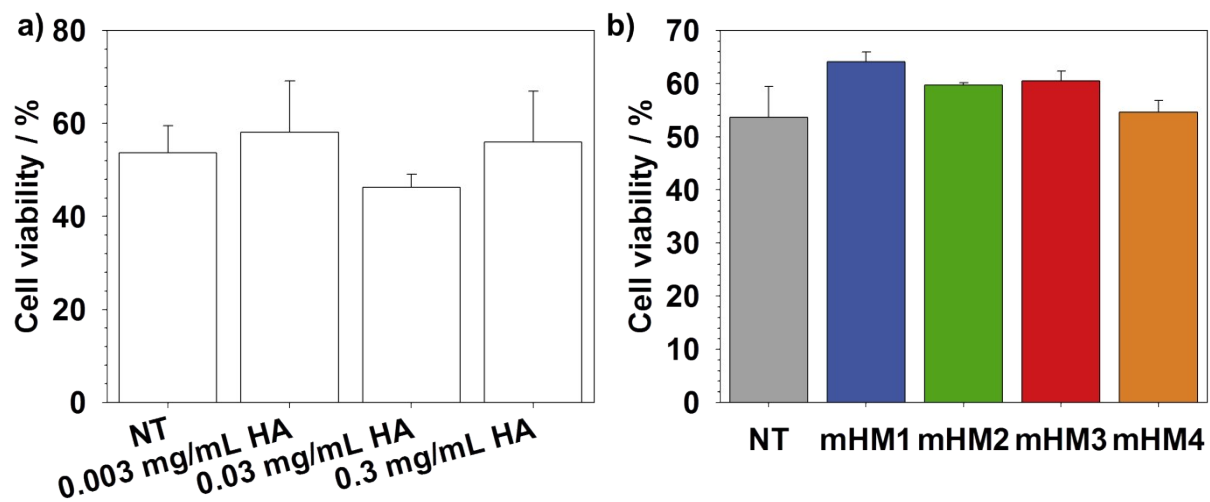


Figure S12. The cell viabilities of MCF-7 cells after treatment of a) different concentrations of HA, b) treatment of mHMs and non-treatment, as a control, followed by addition of 25 μ M of doxorubicin. After 80 h, the cell percentages of live cells were analyzed by MTT assay.

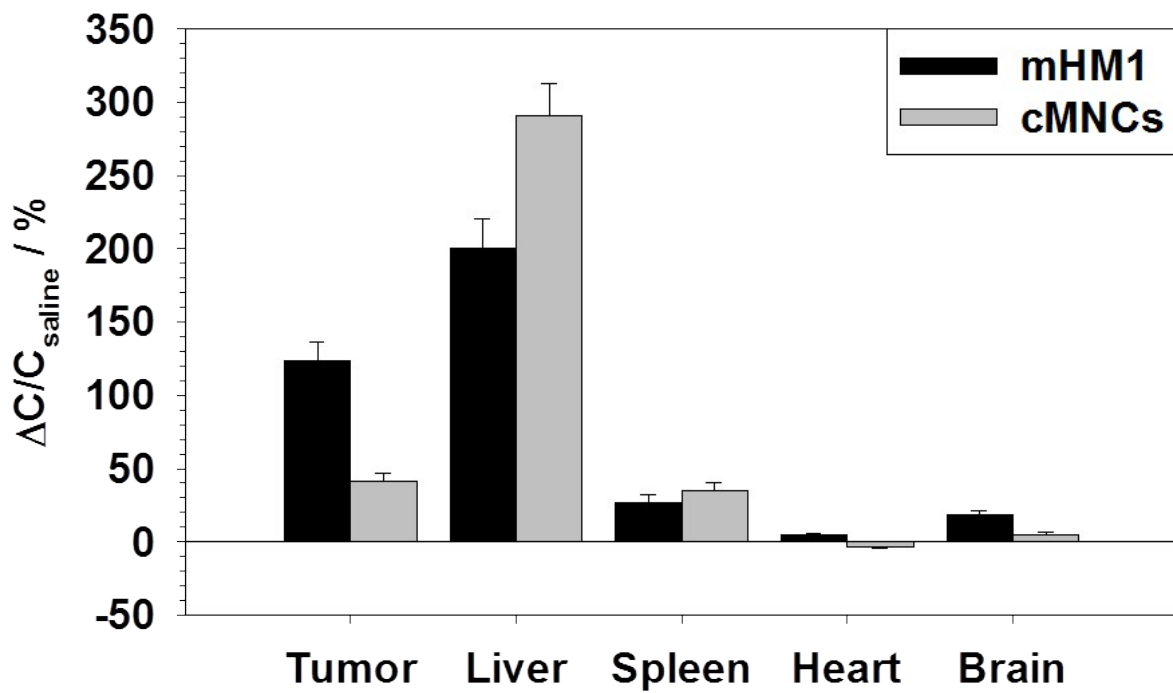


Figure S13. The relative magnetic ion concentrations (%) of bio-distributed mHM1 and cMNCs versus saline were measured based on the amount of MNCs (Fe+Mn) in the organs after treatment using inductively coupled plasma optical emission spectrometry (ICP-OES) analysis (error bars show standard deviation).